Polymer Journal (2019) 51:337–344
https://doi.org/10.1038/s41428-018-0127-6

ORIGINAL ARTICLE

Volume shrinkage of polypeptide hybrid xerogels induced by a helix-sense inversion

Yosuke Mizuno[1] · Hidemine Furuya[1]

Received: 2 July 2018 / Revised: 4 September 2018 / Accepted: 5 September 2018 / Published online: 26 September 2018

Abstract

Poly(L-aspartic acid β-ester) molecules (PAsp) are known for their unique temperature-dependent helix-sense inversion from right- to left-handed helices. This secondary structure transition is expected to switch their mechanical properties, which would allow the development of a stimuli-responsive, solid-state systems of biomaterials. In this work, PAsp hybrid xerogels (PAsp-xgs), which are polymethylmethacrylate xerogels crosslinked by PAsp, were synthesized, and the effects of the PAsp helix-sense inversion on their properties were investigated. PAsp-xg was found to irreversibly shrink to a volume ratio of 0.7 when heated to ~393 K. Notably, the PAsp moieties in the xerogels exhibited a helix-sense inversion at a similar temperature to that of the helix-sense inversion in the homopolymer. These results suggest that the helix-sense inversion induced the volume shrinkage of the PAsp-xgs. All in all, the PAsp-xg synthesized herein is expected to be a new, low environmental load material for stimulus-responsive systems.

Introduction

The application of low environmental load materials is expected to become increasingly important since further reducing the environmental burden caused by materials is required. Biodegradable and biocompatible polymers have attracted a great deal of attention as low environmental load materials [1, 2]. They have been commonly used in medical applications and bioplastics [1–6]. To expand the uses of biodegradable and biocompatible polymers, it is crucial to investigate their functionalization and the subsequent effects arising from such changes.

Synthetic polypeptides, which are a type of biodegradable and biocompatible biopolymers [7–13], are suitable starting materials for these functionalizations because of their unique molecular dynamics, which are expected to be applicable in stimuli-responsive systems. They have been widely investigated owing to their structural similarity to natural proteins that are capable of forming well-defined secondary structures such as helices, sheets, and random coils. In fact, the secondary structures of synthetic polypeptides were reported to change depending on the solvent composition [14–16], temperature [17], and pH [18]. These secondary structure transitions can be used to trigger sol–gel transitions or the transformation of a gel. For example, poly(L-alanine) blocks with a temperature-induced coil–β-sheet transition were used to prepare switchable hydrogels [19]. The formation of a coiled-coil structure induced by changes in the temperature or pH can also serve as a 3D network junction [20]. In fact, Sisido and coworkers have reported an increase in the swelling ratio of a crosslinked polypeptide gel induced by a helix–coil transition [21, 22]. In addition, the groups of Sisido and Inomata have found that crosslinked organogels [23] and hydrogels [24] with highly oriented poly(L-glutamate) derivatives show anisotropic swelling and shrinking behavior induced by a helix–coil transition in the poly(L-glutamate). These deformations of peptide hybrid gels induced by the secondary structure transitions of the polypeptide molecules in the gels are expected to be applicable in actuators, sensors, and drug delivery systems. However, the aforementioned hybrid gels contain a solvent and have weak mechanical properties. Furthermore, for synthetic helical polymers such as polyphenylacetylenes, similar macroscopic shape changes induced by the structural transition of their molecules and self-assembly systems were also reported and extensively

✉ Hidemine Furuya
hfuruya@polymer.titech.ac.jp

[1] School of Materials and Chemical Technology, Tokyo Institute of Technology, 2-12-1-S1-20 Ookayama, Meguro-ku, Tokyo 152-8550, Japan

investigated [25, 26]. However, such transitions may be difficult to achieve in low environmental load materials. Therefore, in an effort to overcome these problems, we focused on poly(L-aspartic acid β-ester) (PAsp).

PAsp is known to exhibit temperature-dependent secondary structure transitions, including a unique helix-sense inversion, not only in solution, but also in a solid state. Moreover, poly(β-phenethyl L-aspartate) (PPLA) undergoes a thermally induced, reversible screw-sense inversion of the α-helix from right to left handed in dilute solutions and lyotropic liquid-crystalline states [27–29]. In particular, Sasaki et al. found that the right-handed α-helix (α_R-helix) of PPLA transforms irreversibly into the left-handed π-helix (π_L-helix) in the solid state at an elevated temperature (413 K) [30]. A helix-sense inversion in the solid state is expected to be a new stimuli-responsive pathway for solid materials, and the properties of the polyaspartate hybrid xerogels are expected to change at the same time as the helix-sense inversions of the polyaspartate molecules in the xerogels.

In this work, we synthesized poly(methyl methacrylate) (PMMA) smart xerogels crosslinked by polyaspartate side chains. As a result, we observed that the dried smart gels (xerogels) shrank after the helix-sense inversion of the polyaspartates in the xerogels. In fact, we proved that this volume shrinkage was induced by the helix-sense inversion of the hybrid xerogels. All in all, with these polypeptide hybrid xerogels, we identified a new means of helix-sense inversion, which should allow the development of low environmental load materials for stimuli-responsive systems.

Experimental procedures

Materials

L-aspartic acid (>99.5%, Wako Chemicals Co., Ltd., Tokyo, Japan), triphosgene (98%, Sigma-Aldrich, MO, USA), triethyl amine (>99.5%, Sigma-Aldrich, MO, USA), 2,2′-azobis(4-methoxy-2,4-dimethylvaleronitrile) (V-70, Wako Chemicals Co., Ltd., Tokyo, Japan), and chloroform (>99%, Nacalai Tesque, Inc., Kyoto, Japan) were used as received. The polymerization inhibitor was removed from ethylene glycol dimethacrylate (EGDM, >97%, TCI, Tokyo, Japan) by washing with a 1 wt% NaOH (>93%, Yoneyama Yakuhin Kogyo Co., Ltd., Osaka, Japan) aqueous solution and subsequent drying with $MgSO_4$ (>99%, Sigma-Aldrich Japan, Tokyo, Japan). Methyl methacrylate (MMA, >99.8%, TCI Tokyo, Japan) was purified by vacuum distillation prior to use. THF was refluxed over CaH_2 (>95%, Wako Chemicals Co., Ltd., Tokyo, Japan) for 6 h and then distilled, while n-hexane was only distilled before use. All other solvents and reactants were reagent grade and were used without further purification.

Synthesis of an aspartate random copolymer with vinyl side chains

β-Phenethyl L-aspartate (PLA) was synthesized through the monoesterification of L-aspartic acid with phenethyl alcohol in the presence of sulfuric acid according to a previously reported procedure [31]. Decyl alcohol, instead of phenethyl alcohol, was used to prepare β-decyl L-aspartate (DLA) following a literature procedure [32]. β-4-Vinyl benzyl L-aspartate (VBLA) was formed by alkylating the L-aspartic acid copper(II) complex with 4-vinyl benzyl chloride based on a procedure previously described by Jeroen Luijten et al. [33]. Then, *N*-carboxyanhydrides (NCA) of the corresponding L-aspartates were synthesized using triphosgene in THF according to a previous report [34]. These NCAs were purified by repeated crystallization from an n-hexane-THF system.

Next, a series of copolymers of PLA or DLA with VBLA were prepared by a standard NCA method [35], and the reaction scheme is shown in Scheme 1. A typical polymerization was conducted in the following way. The polymerization of PLA-NCA (0.79 g, 3.00 mmol) and VBLA-NCA (0.09 g, 0.33 mmol) was carried out in chloroform (>99%) using triethyl amine as an initiator with a molar ratio of NCA to initiator (A/I ratio) of 100. The reaction mixture was stirred for 6 d at room temperature, after which the polymer was purified by precipitation in excess methanol. The polymer was then isolated by filtration through a glass filter and dried in vacuo. Poly(PLA-*co*-VBLA) (PPLA-VBLA) was thus obtained as a white fibrous solid (Mw = *ca.* 22,000 by viscosity measurement [36]). The mole fraction of PPLA-VBLA as measured by ^{1}H NMR was found to be PLA/VBLA = 9/1: ^{1}H NMR (400 MHz, $CDCl_3$/TFA): δ(ppm) = 2.72–3.00 (3.8H, >CHCH_2COO– and –COOCH$_2$CH_2Ph), 4.11–4.39 (1.8H, –COOCH_2CH$_2$–), 4.81–5.11 (1.2H, –COOCH_2Ph– and –NHC*H*CO–), 5.11–5.29 (0.1H, vinyl), 5.57–5.77 (0.1H, vinyl), 6.51–6.72 (0.1H, vinyl), 7.76–8.12 (1H, N*H*).

The A/I ratio for the synthesis of poly(DLA-*co*-VBLA) (PDLA-VBLA) was 125, and the polymerization of PDLA-VBLA was carried out over 7 d. Finally, PDLA-VBLA was obtained as a white fibrous solid (Mw = *ca.* 32,000 [36]) with a mole fraction DLA/VBLA of 9/1: ^{1}H NMR (400 MHz, $CDCl_3$/TFA): δ(ppm) = 0.65–0.98 (2.7H, –CH_3), 0.98–1.46 (10.8H, –C$_6H_{12}$CH$_3$), 1.46–1.72 (3.6H, –COOCH$_2$CH_2CH_2–), 2.76–3.16 (2H, >CHCH_2COO–), 3.83–4.29 (1.8H, –COOCH_2CH$_2$–), 4.75–5.19 (1.2H, –NHC*H*CO– and –COOCH_2Ph–), 5.19–5.36 (0.1H, vinyl), 5.59–5.77 (0.1H, vinyl), 6.57–6.80 (0.1H, vinyl), 7.82–8.24 (1H, N*H*).

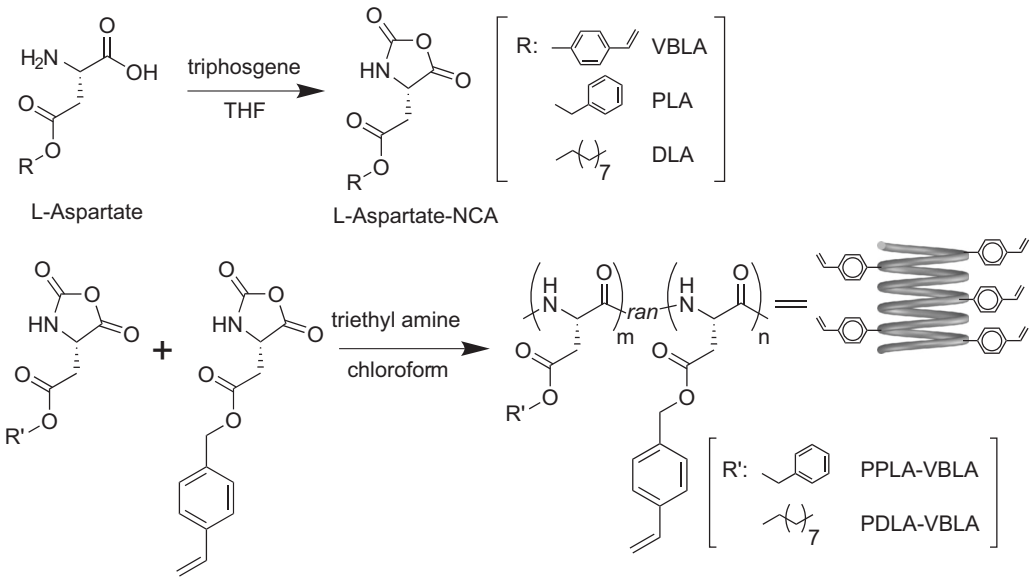

Scheme 1 Synthesis of an aspartate random copolymer with vinyl side chains

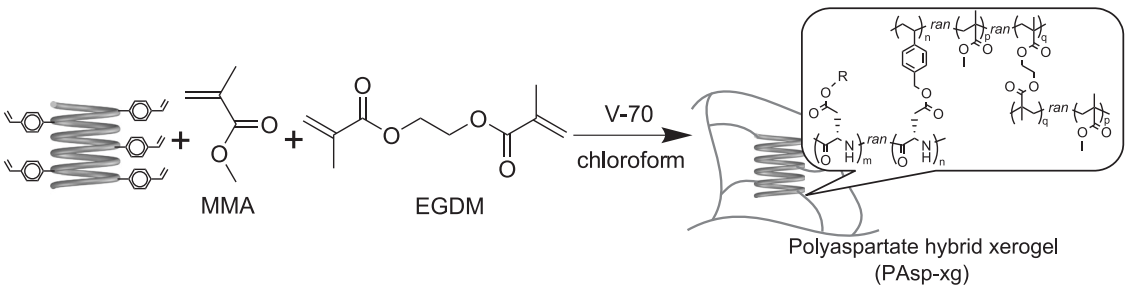

Scheme 2 Synthesis of a polyaspartate hybrid xerogel

Synthesis of polyaspartate hybrid xerogel sheets

A typical procedure for the preparation of a polyaspartate hybrid xerogel is described below, and a reaction scheme is shown in Scheme 2. First, PPLA-VBLA (100 mg) was dissolved in chloroform (12 ml). This solution was then mixed with MMA (2.0 ml, 14.08 mmol) and EGDM (0.2 ml, 1.06 mmol) and purged with nitrogen gas for 10 min. V-70 (46 mg, 0.15 mmol) was added to the mixture as a radical initiator, after which the solution was heated to 323 K in a Teflon mold (size: length = 16 mm, width = 16 mm, and height = 1 mm) and left to react for 1 d. The most suitable condition of polymerization was determined by the examination of several temperatures and radical initiators (V-70 or AIBN). The obtained gel was swelled in chloroform for 1 d to remove the residue. Finally, the PMMA xerogel crosslinked by PPLA-VBLA (hereafter referred to as PPLA-xg) was obtained by repeated solvent substitution using a mixture of chloroform and methanol as solvent with subsequent vacuum drying. The xerogel crosslinked by PDLA-VBLA (hereafter referred to as PDLA-xg) was synthesized via a similar procedure using 75 mg of PDLA-VBLA and 6 ml of chloroform while maintaining constant the ratios of the moles of other reagents to the weight of the PDLA-VBLA. Additionally, a PMMA xerogel crosslinked only by EGDM (hereafter referred to as PMMA-xg) was also prepared using the same procedure as that used for PPLA-xg without the use of PPLA-VBLA.

Characterization

^{1}H NMR spectra were recorded on a JNM-AL400 spectrometer (JEOL, Ltd., Tokyo, Japan) operated at 400 MHz. The ^{1}H NMR measurements were acquired in a mixed solution of deuterated chloroform and trifluoroacetic acid at 298 K using tetramethylsilane (TMS) as an internal reference. The examination of the volume change of the xerogel sheets depending on the annealed temperature was carried out as follows. The rectangular sheets of the xerogel were heated stepwise on a hot plate, starting from 303 K and then every 10 K from 353 to 453 K with a retention time

for each annealing point of 1 h. The length ratio, R, of the sides of the sheet was then measured after each annealing point. The volume ratio, V, of the sheets was estimated by Eq. (1) in the isotropic change of shape:

$$V = R^3 \quad (1)$$

where $R = L/L_0$: L and L_0 are the length of sides of the sample at a given annealing temperature and at 303 K, respectively.

The FT-IR spectra of the xerogel samples were obtained on an FT/IR-4100 (JASCO Co., Tokyo, Japan) at room temperature by using KBr pellets. Before preparing the pellets, the xerogels were heated on a hot plate from room temperature to 443 K. Additionally, the FT-IR spectra of the PPLA homopolymer solid film casted on a Si substrate were measured at room temperature.

Solid-state ^{13}C NMR measurements were performed by cross-polarization (CP)/magic angle spinning (MAS) at room temperature using an Avance DSX300 (Bruker Co., MA, USA) spectrometer operating at 75.47 MHz. A dipolar decoupling (DD)/MAS method was carried out in the temperature range of 373-413 K. Samples were spun at 6.5–8 kHz. The contact and repetition times were 2 ms and 1 s, respectively, and the spectra were accumulated 480–1280 times. In the ^{13}C NMR measurements via the CP/MAS method, spinning sidebands appearing due to an insufficient spinning rate were removed via the total suppression of the sidebands (TOSS) method.

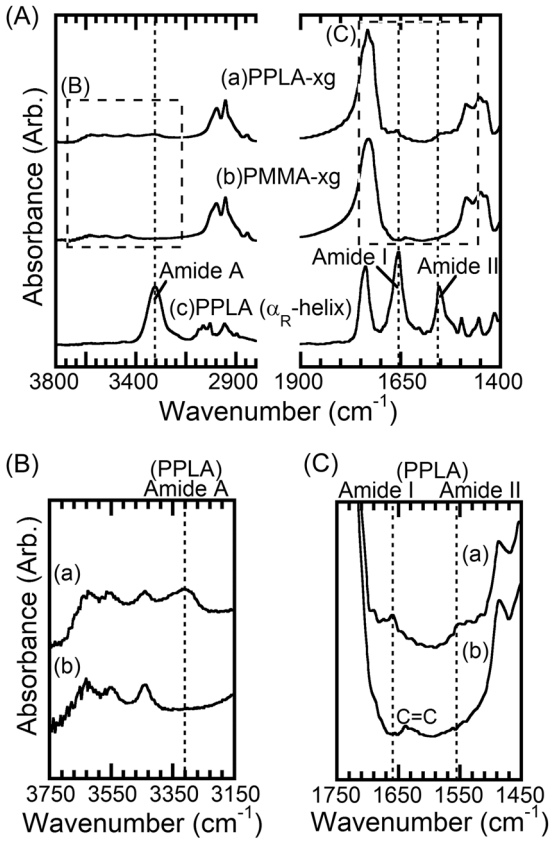

Fig. 1 **A** FT-IR spectra of **a** PPLA-xg, **b** PMMA-xg, and **c** PPLA. **B** Enlarged IR spectra of PPLA-xg and PMMA-xg around their amide A band. **C** Enlarged IR spectra of PPLA-xg and PMMA-xg around their amide I and amide II bands

Results and discussion

Synthesis of polyaspartate hybrid xerogels

Figure 1 shows the IR spectra of PPLA-xg, PMMA-xg, and the PPLA homopolymer in the solid state at room temperature. Three characteristic weak infrared absorptions at 1550, 1659, and 3317 cm^{-1} were observed in the spectrum of PPLA-xg. The absorption bands at 1550 and 3317 cm^{-1} were obtained by a waveform separation, as shown in Fig. 1B, C. In contrast, no peaks near the positions of the aforementioned three bands were observed in the spectrum of PMMA-xg, except for an absorption at 1640 cm^{-1}, which was assigned to the vinyl groups. After substantial analysis, the three absorption bands at 1550, 1659, and 3317 cm^{-1} were attributed to the amide II, amide I, and amide A bands of the PPLA homopolymer, which formed an α_R-helix in the solid state [30]. These results show that the PPLA molecules were successfully crosslinked with the PMMA gel network to form an α_R-helix at room temperature even in the xerogel network. Notably, the position of the amide A band for PPLA-xg was slightly different from that of the PPLA homopolymer (3298 cm^{-1}). This difference could be due to the moisture in the xerogel and the suppression of the molecular mobility of PPLA by the crosslinked structure. Additionally, as shown in Fig. 1B, an overtone band of the C=O stretch, which was derived from PMMA, and two bands originating from moisture were observed in the 3350–3800 cm^{-1} region [37, 38].

Volume shrinkage of polyaspartate hybrid xerogels upon heating

Figure 2 shows the temperature dependence of the volume ratios of PPLA-xg and PMMA-xg. Below 393 K, the volume of PPLA-xg was similar to that of PMMA-xg. However, these xerogels shrank slightly at ~373 K, which is the glass transition temperature of PMMA [39]. It was assumed that the slight shrinkage was due to the release of residual stress in the xerogel networks. In contrast, PPLA-xg shrank suddenly at ~393 K, after which the volume ratio changed to 0.69. Notably, the hybrid xerogel shrank more than PMMA-xg. The difference in the shrinkage behavior of these xerogels indicates the significant shrinkage was caused by the PPLA that was crosslinked with the xerogel

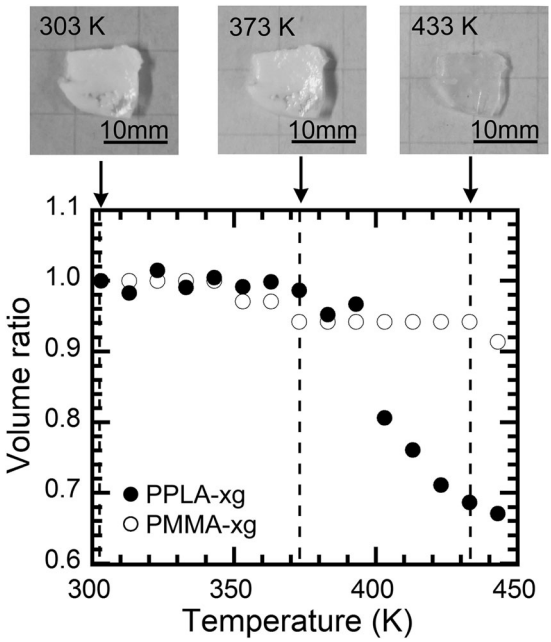

Fig. 2 Temperature dependence of the volume ratios of PPLA-xg (filled circles) and PMMA-xg (open circles)

networks. Moreover, the temperature at which the volume reduction took place was similar to the helix transition temperature of the PPLA homopolymer. Considering these results, we could assume that the helix-sense inversion of the main chain of PPLA in the xerogels induced the shrinkage of PPLA-xg.

Secondary structure of PPLA crosslinked with the xerogel network

The temperature dependence of the amide I band positions for the annealed samples of PPLA-xg is shown in Fig. 3. The band for PPLA-xg annealed at 393 K was observed at ~1658 cm^{-1}, which corresponded to the α_R-helix [30]. In contrast, at an annealing temperature of 403 K, two peaks corresponding to the amide I band were observed, which indicates that the PPLA molecule in the xerogel was able to form an α_R-helix until 403 K. Above 413 K, only one peak (1674 cm^{-1}) was detected for the amide I band. Moreover, at this temperature, the amide A band shifted from 3317 to 3335 cm^{-1}. The amide I and amide A bands at 1674 and 3335 cm^{-1} correspond to the left-handed π_L-helix in the solid state [30]. Therefore, it was concluded that PPLA in PPLA-xg exhibited an irreversible helix-sense inversion from an α_R-helix to a π_L-helix at ~403 K. However, the amide II band in the spectra did not seem to change at all as the annealing temperature increased. This, in turn, did not match the shift in the amide II band of the PPLA homopolymer from 1553 to 1536 cm^{-1} that occurred around the temperature of the helix-sense inversion [30].

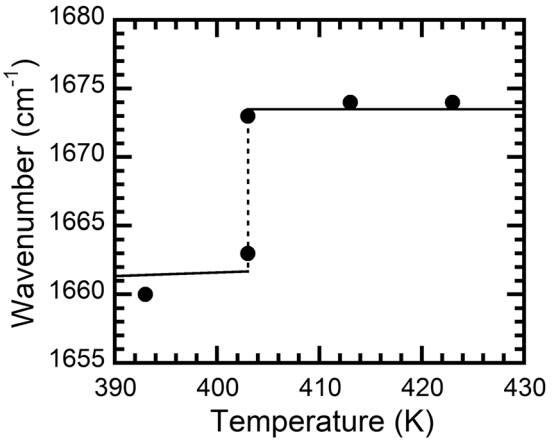

Fig. 3 Temperature dependence of the peak position of the amide I bands of PPLA-xg

Because the intensity of the amide II band was much weaker than those of other characteristic absorption bands for PPLA and the peak of the moisture overlapped with the amide II band, a change in the amide II band of PPLA-xg was not detected.

The xerogel prepared only using PPLA molecules, which exhibited a similar shrinking behavior to PPLA-xg, was also analyzed by ^{13}C NMR spectroscopy. The ^{13}C chemical shift of the β-proton of the side chains of PPLA in PPLA-xg at 303 K was observed at 34.5 ppm, while at 413 K, the resonance shifted to 35.8 ppm. Considering the chemical shift assignments for the helical structures [40], the ^{13}C NMR spectra indicated that the PPLA molecules cross-linked with the PMMA chains to form an α_R-helix at 303 K, which transformed to a π_L-helix at 413 K. Notably, the results of the NMR measurements are consistent with those from the IR measurements of PPLA-xg. Therefore, we can conclude that the PPLA in PPLA-xg underwent an irreversible helix-sense inversion from an α_R-helix to a π_L-helix at 403 K. Moreover, the observed temperature of the helix-sense inversion was the same as the initiation temperature of the shrinking behavior of PPLA-xg. These results suggest that the helix-sense inversion of PPLA-xg induced the volume reduction of PPLA-xg.

Hybrid xerogel with polyaspartates bearing long alkyl side chains

Figure 4 shows the temperature dependence of the volume ratio of PDLA-xg, which contained PDLA bearing decyl groups in its side chains. Additionally, the figure displays the temperature dependence of the position of the amide I band of PDLA in the xerogels. The amide I band of PDLA-xg was observed at ~1660 cm^{-1} for an annealing temperature of 383 K or lower. In contrast, for samples annealed at 393 K or higher, the position of this band shifted to *ca.*

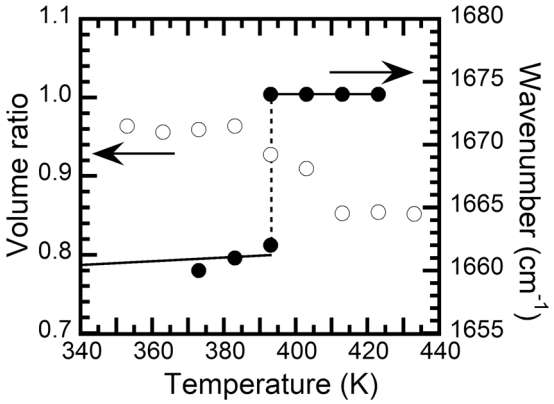

Fig. 4 Temperature dependence of the volume ratio (open circles) and peak positions of the amide I bands (filled circles) of PDLA-xg

1674 cm^{-1}. Notably, peak shifts for the amide A and amide II bands of the PDLA molecules in the xerogels could not be detected due to the absorbance peaks of moisture. The shifts of the amide I band of PDLA indicated that the PDLA in PDLA-xg underwent an irreversible helix-sense inversion from an α_R-helix to a π_L-helix at 393 K. This transition behavior was similar to that of the PDLA homopolymer in the solid state [32]. In addition, volume shrinkage of PDLA-xg was observed in the temperature range of 393–413 K (Fig. 4). The onset temperature of the shrinkage of PDLA-xg corresponded to the temperature of the helix-sense inversion of PDLA in the xerogel. Since the temperature of the helix-sense inversion of PDLA is close to the glass transition temperature of PMMA, the shrinkage of PDLA-xg seems slower than that of PPLA-xg. Finally, when the shrinkage of PDLA-xg was complete (413 K), the volume ratio was estimated to be 0.85. This volume reduction was slightly smaller than that of PPLA-xg.

The mechanisms of shrinkage of the polyaspartate hybrid xerogels

The polyaspartate hybrid xerogels were found to shrink substantially after the helix-sense inversion of their polyaspartates regardless of the side chain structures on the polyaspartates. This observation suggests that the helix-sense inversions of the main chain of polyaspartates in the xerogels induced the shrinkage of these xerogels. As a result, PDLA and PPLA in the xerogels exhibited an irreversible helix-sense inversion from an α_R-helix to a π_L-helix. As previously reported, the unit height of the α_R-helix is 1.50 Å, while that of the π_L-helix is 1.17 Å [41–44]. Therefore, the helix height of the aforementioned polyaspartates became ~20% shorter after the helix-sense inversion. On the other hand, the radius of their helix structures increased by ~20% after the transition, since the radius of the α_R-helix and π_L-helix were 2.3 Å and 2.8 Å, respectively [41–45]. With this characteristic transformation of the helical structure, the occupied volume of the main chain after the transition increased by a factor of 1.15. Moreover, the observed density of the PPLA homopolymer in the solid state decreases after the helix-sense inversion [30]. Based on these facts, the helix-sense inversions of the PPLA and PDLA homopolymers were assumed to contribute to the increase in their volumes. Therefore, the volumes of the hybrid xerogels were also supposed to increase after the transition. However, the hybrid xerogel shrank, and the volume ratio decreased significantly after the helix-sense inversion. This unexpected result implies that the change in the length along the helical axis may strongly contribute to the volume transition of the hybrid xerogels. Generally, the length of the side chains is greater than the radius of the helix [46]. In addition, the side chains reportedly have various conformations, while the main chains show specific helical conformations, indicating that the side chains are more flexible than the main chains [29, 47, 48]. The change in the length of the helix in the vertical direction (along the helical axis) appeared to only slightly affect the volume of the xerogels. Considering these results, the shrinkage mechanism of the PAsp hybrid xerogels can be described as follows. Since the helix-sense inversion temperature was higher than the glass transition temperature of PMMA [39], the PMMA chains were able to move easily in response to any stress in the transition. In association with the contraction of the helix along the helical axis, the polyaspartate molecules in the xerogels pulled the PMMA chains that were crosslinked with each other. Then, each PMMA chain was drawn toward the corresponding PAsp molecule. Therefore, the PAsp hybrid xerogels shrank through a series of interactions between these molecules in the hybrid xerogels. However, the aforementioned proposed shrinkage mechanism has not yet been evaluated in detail. The volume ratios of PPLA-xg and PDLA-xg were different after shrinkage, although these xerogels contained almost the same amounts of polyaspartate molecules. We prepared PPLA hybrid xerogels without EGDM in our preliminary study [49]. The PPLA xerogels with and without EGDM were observed to shrink to volume ratios of 0.69 and 0.95, respectively. The helix-sense inversion of PPLA was observed in the PPLA hybrid xerogels with and without EGDM. Comparing the results of the PPLA hybrid xerogels with and without EGDM to that of PMMA-xg, the presence of both PPLA and EGDM seems to cause a large volume shrinkage. The second crosslinking EGDM molecule may be involved in propagating the change of the helix structure more efficiently within the sample shape. Other factors for the shrinkage of the polyaspartate hybrid xerogels, such as the crosslink density of the xerogel network and the microstructure of the xerogels, should also be considered when clarifying the mechanism.

In summary, we present the formation of polypeptide hybrid xerogels in which the PAsp molecules exhibited a helix-sense inversion. Moreover, the shrinking behavior upon heating was observed in the solid state for the first time. As a result, we found that the temperature of the volume reduction was consistent with the temperature of the helix-sense inversion. In addition, the shrinking behavior was observed to be independent of the structure of the side chains on PAsp. Therefore, it is reasonable to conclude that the helix-sense inversion induced the shrinkage of the xerogel. The decrease in the helix length in the direction of the helical axis was considered a major factor in the shrinking behavior. However, further investigation into the effects of the gel structure on the shrinkage is needed to clarify the mechanism. All in all, we believe that if the shrinkage temperature and scale can be tuned, this system has the potential to allow for the development of a new, low environmental load actuator.

Acknowledgements We would like to thank Editage (www.editage.jp) for the English language editing.

Compliance with ethical standards

Conflict of interest The authors declare that they have no conflict of interest.

References

1. Gupta AP, Kumar V. New emerging trends in synthetic biodegradable polymers – polylactide: a critique. Eur Polym J. 2007;43:4053–74.
2. Scarfato P, Di Maio L, Incarnato L. Recent advances and migration issues in biodegradable polymers from renewable sources for food packaging. J Appl Polym Sci. 2015;132:42597.
3. Khan W, Hosseinkhani H, Ickowicz D, Hong P-D, Yu D-S, Domb AJ. Polysaccharide gene transfection agents. Acta Biomater. 2012;8:4224–32.
4. Luten J, van Nostrum CF, De Smedt SC, Hennink WE. Biodegradable polymers as non-viral carriers for plasmid DNA delivery. J Control Release. 2008;126:97–110.
5. Middleton JC, Tipton AJ. Synthetic biodegradable polymers as orthopedic devices. Biomaterials. 2000;21:2335–46.
6. Iwata T. Biodegradable and bio-based polymers: future prospects of eco-friendly plastics. Angew Chem Int Ed. 2015;54:3210–5.
7. Ohkawa K, Kitsuki T, Amaike M, Saitoh H, Yamamoto H. Biodegradation of ornithine-containing polylysine hydrogels. Biomaterials. 1998;19:1855–60.
8. Ohkawa K, Shoumura K, Shirakabe Y, Yamamoto H. Photoresponsive peptide and polypeptide systems 15*: synthesis of photo-crosslinkable poly(amino acid)s by watery process and its application as a reinforcement for polyion complex fibers. J Mater Sci. 2003;38:3191–7.
9. Ohkawa K, Shoumura K, Yamada M, Nishida A, Shirai H, Yamamoto H. Photoresponsive peptide and polypeptide systems, 14. Biodegradation of photocrosslinkable copolypeptide hydrogels containing L-ornithine and δ-7-coumaryloxyacetyl-L-ornithine residues. Macromol Biosci. 2001;1:149–56.
10. Itaka K, Ishii T, Hasegawa Y, Kataoka K. Biodegradable polyamino acid-based polycations as safe and effective gene carrier minimizing cumulative toxicity. Biomaterials. 2010;31:3707–14.
11. Yoshida H, Klinkhammer K, Masusaki M, Möller M, Klee D, Akashi M. Disulfide-crosslinked electrospun poly(γ-glutamic acid) nonwovens as reduction-responsive scaffolds. Macromol Biosci. 2009;9:568–74.
12. Hsieh C-Y, Tsai S-P, Wang D-M, Chang Y-N, Hsieh H-J. Preparation of γ-PGA/chitosan composite tissue engineering matrices. Biomaterials. 2005;26:5617–23.
13. Thombre SM, Sarwade BD. Synthesis and biodegradability of polyaspartic acid: a critical review. J Macromol Sci Part A. 2005;42:1299–315.
14. Doty P, Holtzer AM, Bradbury JH, Blout ER. Polypeptides. II. The configuration of polymers of γ-benzyl-L-glutamate in solution. J Am Chem Soc. 1954;76:4493–4.
15. Doty P, Bradbury JH, Holtzer AM. Polypeptides. IV. The molecular weight, configuration and association of poly-γ-benzyl-L-glutamate in various solvents. J Am Chem Soc. 1956;78:947–54.
16. Blout ER, Idelson M. Polypeptides. VI. Poly-α-L-glutamic acid: preparation and helix-coil conversions. J Am Chem Soc. 1956;78:497–8.
17. Doty P, Yang JT. Polypeptides. VII. Poly-γ-benzyl-L-glutamate: the helix-coil transition in solution. J Am Chem Soc. 1956;78:498–500.
18. Doty P, Wada A, Yang JT, Blout ER. Polypeptides. VIII. Molecular configurations of poly-L-glutamic acid in water-dioxane solution. J Polym Sci. 1957;23:851–61.
19. Oh HJ, Joo MK, Sohn YS, Jeong B. Secondary structure effect of polypeptide on reverse thermal gelation and degradation of L/DL-poly(alanine)–poloxamer–L/DL-poly(alanine) copolymers. Macromolecules. 2008;41:8204–9.
20. Petka WA, Harden JL, McGrath KP, Wirtz D, Tirrell DA. Reversible hydrogels from self-assembling artificial proteins. Science. 1998;281:389–92.
21. Kishi R, Sisido M, Tazuke S. Liquid-crystalline polymer gels. 1. Cross-linking of poly(γ-benzyl L-glutamate) in the cholesteric liquid-crystalline state. Macromolecules. 1990;23:3779–84.
22. Matsuoka Y, Kishi R, Sisido M. Liquid-crystalline polymer gels VI. Preparation and swelling behavior of cross-linked hydrogels of poly(L-glutamic acid) possessing cholesteric order. Polym J. 1993;25:919–27.
23. Kishi R, Sisido M, Tazuke S. Liquid-crystalline polymer gels. 2. Anisotropic swelling of poly(γ-benzyl L-glutamate) gel cross-linked under a magnetic field. Macromolecules. 1990;23:3868–70.
24. Inomata K, Iguchi Y, Mizutani K, Sugimoto H, Nakanishi E. Anisotropic swelling behavior induced by helix–coil transition in liquid crystalline polypeptide gels. ACS Macro Lett. 2012;1:807–10.
25. Percec V, Rudick JG, Peterce M, Heiney PA. Nanomechanical function from self-organizable dendronized helical polyphenylacetylenes. J Am Chem Soc. 2008;130:7503–8.
26. Yashima E, Ousaka N, Taura D, Shimomura K, Ikai T, Maeda K. Supramolecular helical systems: helical assemblies of small molecules, foldamers, and polymers with chiral amplification and their functions. Chem Rev. 2016;116:13752–990.
27. Abe A, Okamoto S, Kimura N, Tamura K, Onigawara H, Watanabe J. Helix-helix transition of α-helical poly(β-phenethyl L-aspartate) observed in the lyotropic liquid-crystalline state. Acta Polym. 1993;44:54–56.
28. Watanabe J, Okamoto S, Abe A. A novel transition in the lyotropic cholesteric mesophase induced by the helix sense inversion of α-helical poly(β-phenethyl L-aspartate). Liq Cryst. 1993;15:259–63.
29. Abe A, Furuya H, Okamoto S. Spatial configurations, transformation, and reorganization of mesophase structures of

polyaspartates—a highly intelligent molecular system. Biopolymers. 1997;43:405–12.
30. Sasaki S, Yasumoto Y, Uematsu I. π-Helical conformation of poly (β-phenethyl L-aspartate). Macromolecules. 1981;14:1797–801.
31. Goodman M, Listowsky I, Schmitt EE. Conformational aspects of polypeptides. V. Molar rotational model compounds for poly-γ-methyl L-glutamate. J Am Chem Soc. 1962;84:1296–303.
32. Sakajiri K. Reversible helix-helix transition involving a screw sense inversion in the solid state of polyaspartates. Tokyo: Ph.D. Thesis, Tokyo Institute of Technology; 2000.
33. Luijten J, Groeneveld DY, Nijboer GW, Vorenkamp EJ, Schouten AJ. Cross-linking-induced permanently perpendicular helix orientation in surface-grafted polyglutamate films. Langmuir. 2007;23:8163–9.
34. Daly WH, Poché D. The preparation of N-carboxyanhydrides of α-amino acids using bis(trichloromethyl)carbonate. Tetrahedron Lett. 1988;29:5859–62.
35. Bradbury EM, Carpenter BG, Stephens RM. Conformational studies of polymers and copolymers of L-aspartate esters. II. Infrared studies and the factors involved in the formation of the ω-helix. Biopolymers. 1968;6:905–15.
36. Hayashi Y, Teramoto A, Kawahara K, Fujita A. Solution properties of synthetic polypeptides. V. Helix–coil transition in poly(β-benzyl-L-aspartate). Biopolymers. 1969;8:403–20.
37. Gilbert AS, Pethrick RA, Phillips DW. Acoustic relaxation and infrared spectroscopic measurements of the plasticization of poly(methyl methacrylate) by water. J Appl Polym Sci. 1977; 21:319–30.
38. Sutandar P, Ahn DJ, Franses EIM. FTIR ATR analysis for microstructure and water uptake in poly(methyl methacrylate) spin cast and Langmuir-Blodgett thin films. Macromolecules. 1994;27: 7316–28.
39. Beevers RB, White EFT. Physical properties of vinyl polymers. Part 1.—Dependence of the glass-transition temperature of polymethylmethacrylate on molecular weight. Trans Faraday Soc. 1960;56:744–52.
40. Abe A, Maeda Y, Furuya H, Hiromoto A, Kondo T. Thermodynamic studies on the helix-sense inversion of polyaspartates in the solid state. Polymer. 2012;53:2673–80.
41. Pauling L, Corey RB. Atomic coordinates and structure factors for two helical configurations of polypeptide chains. Proc Natl Acad Sci USA. 1951;37:241–50.
42. Low BW, Grenville-Wells HJ. Generalized mathematical relationships for polypeptide chain helices. The coordinates of the Π helix*. Proc Natl Acad Sci USA. 1953;39:785–801.
43. Low BW, Baybutt RB. The π helix—a hydrogen bonded configuration of the polypeptide chain. J Am Chem Soc. 1952;74: 5806–7.
44. Donohue J. Hydrogen bonded helical configurations of the polypeptide chain. Proc Natl Acad Sci USA. 1953;39:470–8.
45. Schulz GE, Schirmer RH. Patterns of folding and association of polypeptide chains. In: Schulz GE, Schirmer RH, editors. Principles of protein structure. New York: Springer-Verlag; 1979. Ch. 5, p. 66-107.
46. Wieringa RH, Siesling EA, Werkman PJ, Angerman HJ, Vorenkamp EJ, Schouten AJ. Surface grafting of poly(L-glutamates). 2. Helix orientation. Langmuir. 2001;17:6485–90.
47. Abe A, Yamazaki T. Deuterium NMR analysis of poly(γ-benzyl L-glutamate) in the lyotropic liquid-crystalline state: orientational order of the α-helical backbone and conformation of the pendant side chain. Macromolecules. 1989;22:2138–45.
48. Okamoto S, Furuya H, Abe A. Conformational analysis of α-helical polypeptides in two opposite screw forms. A combined use of ^{2}H NMR and MD simulation. Polym J. 1995;27:746–56.
49. Mizuno Y. Helix-sense inversion behavior and volume change of polypeptide hybrid gels. Tokyo: Master Thesis, Tokyo Institute of Technology; 2016.